ABSTRACT

SZCZEPANSKI, AUBREE ANN. Copepod-microplankton Dynamics in the Northern Gulf of Mexico. (Under the direction of Dr. Astrid Schnetzer).

Copepods play pivotal roles for energy transfer from primary producers to higher trophic levels, they impact phytoplankton and microzooplankton standing stocks and commonly affect prey community structure through grazing. This study examined spatiotemporal trends in microplankton-copepod trophic dynamics in the northern Gulf of Mexico (nGOM). Changes in prey abundances and community structure were studied at onshore (inner shelf) and offshore sites (continental slope) during July/August 2017, October 2017, January 2018 and March 2018. Carbon-based relative contributions from heterotrophic/mixotrophic dinoflagellates and ciliates to copepod diet repeatedly exceeded those from diatoms and fell within ranges typically reported for oligotrophic systems. Ingestion rates (IR) increased linearly with prey abundance indicating that copepod consumption was constrained by food availability. Daily average estimates on removal of ciliate, diatom and dinoflagellate standing stocks (15 – 200 µm size fraction) varied markedly and indicated that protist populations were strongly impacted by copepod grazing activity (mean = 38% and range from <1 to 134%). Comparison among study sites showed that protistan community structure, copepod diet composition and biomass removal rates differed spatially (i.e., among on and shore locations) while season had much less or no impact on these factors. The findings in this study emphasize the importance of spatial variations in protistan-copepod trophic interactions within the nGOM.

Copepod-microplankton Dynamics in the Northern Gulf of Mexico

by
Aubree Ann Szczepanski

A thesis submitted to the Graduate Faculty of
North Carolina State University
in partial fulfillment of the
requirements for the degree of
Master of Science

Marine, Earth, and Atmospheric Sciences

Raleigh, North Carolina
2019

APPROVED BY:

_____	_____
Astrid Schnetzer Committee Chair	David Eggleston
_____	_____
Blake Schaeffer	Beth Stauffer External Member

DEDICATION

This thesis is dedicated to my parents that have been my main support system throughout my thesis.

BIOGRAPHY

I grew up in the Great Lake State of Michigan. My travels have taken me to the ocean. I have experienced the opportunities and benefits that water environments offer. My appreciation of small ponds, tributaries, lakes, Great Lakes and oceans helped direct me to my current studies and passion for research. I decided to study the relationship between ecosystems and organisms within them.

ACKNOWLEDGMENTS

Thank you to the committee for their thoughtful consideration of my report. A special thanks goes to Dr. Schnetzer for her continued support and guidance in the completion of this thesis. Thank you for my committee members Dr. Beth Stauffer, Dr. David Eggleston, and Dr. Blake Schaeffer for their guidance throughout my thesis. I would like to acknowledge my fellow lab members whose supportive comments and collaborative sample collections helped make this possible. Also thank you to the crew of R/V Pelican, RAPID collaborators, and their team members. This study was partially supported through funds from the National Science Foundation RAPID grant (OCE-1760465).

TABLE OF CONTENTS

LIST OF TABLES

LIST OF FIGURES

`

Introduction:

Copepods are the most numerous mesozooplankton within the oceans (200 – 2,000 µm in size), typically making up 70 - 90% of the assemblage (Turner 2004). Copepods are a major trophic (carbon) link between phytoplankton and upper-level consumers (from fish to whales) (Saiz & Calbet 2011). For example, given a total of 50 gigatons of primary productivity a year (Gt C yr^{-1}), copepods consume up to 18 Gt C yr^{-1} of phytoplankton biomass and ~11 Gt C yr^{-1} preying on microzooplankton (e.g., ciliates and heterotrophic dinoflagellates) with the remainder being grazed by microzooplankton (Calbet 2008, Steinberg & Landry 2017). Despite the central biogeochemical roles that copepods play, resolving the nature of microplankton-copepod dynamics often presents a daunting task factoring in the enormous diversity within prey populations and the variety of feeding modes employed by metazoan grazers and/or varying life stages (Blaxter et al. 1998). Deciphering these trophic interactions is required to inform estimates of energy flux and carbon export within the ocean (Steinberg & Landry 2017).

Several approaches have been employed to investigate natural copepod diets including chemical biomarkers (e.g., chlorophyll a (chl *a*), fatty acids or stable isotopes) (e.g., Lichti et al. 2017) gut content analyses (e.g., Schnetzer & Steinberg 2002, Kleppel et al. 1988) or prey-specific molecular markers (e.g., Troedsson et al. 2009, Durbin, 2008). Microscopy is another widely-used method to examine how major taxonomic groups (e.g., diatoms, ciliates or dinoflagellates) contribute to crustacean diets (e,g., Schnetzer & Caron 2005, López & Anadón 2008, Saiz & Calbet 2011). Most copepods feed as omnivores and have the ability to switch between prey items as food environments and metabolic requirement change (Kleppel 1993, Steinberg & Landry 2017). As far as feeding selection goes, microzooplankton are commonly the preferred

food, even if phytoplankton are the most abundant prey (Fessenden & Cowles 1994, Broglio et al. 2004).

Comprehensive reviews of feeding studies from a range of trophic environments show the importance of microzooplankton contributions to copepod diet, especially in less productive systems (Calbet 2001, Saiz & Calbet 2011). In these environments, smaller phytoplankton typically dominate (~5 µm or less) and these algae, due to their size, cannot be consumed as efficiently by copepods (Hansen et al. 1994). Here, ciliates and dinoflagellates may remove up to ~75% of primary production (Berggreen et al. 1988) making the microzooplankton-copepod trophic link key for carbon flow to upper trophic levels (e.g. Calbet et al. 2004). In productive systems, this link is weaker and larger phytoplankton, such as diatoms, are considered equally important prey for copepods (Saiz & Calbet 2011). Knowledge on how copepod diet and carbon ingestion rates change across trophic gradients is key for estimates of biogeochemical fluxes within marine systems (Sherr & Sherr 2007).

Nearshore waters within the northern Gulf of Mexico (nGoM) are strongly impacted by coastal runoff which supports high primary productivity, while most of the offshore waters (along and beyond the outer continental shelf) are characterized by oligotrophic conditions and low productivity (Mendelssohn et al. 2017). These on- to offshore gradients in primary productivity can be especially pronounced along the continental shelf of the northwest/central Gulf of Mexico where access nutrient runoff from the Mississippi regularly results in severe oxygen depletion (‘dead zones’) during the summer months (Rabalais et al. 2002). The present study characterized spatiotemporal patterns in microplankton community structure, copepod abundance and their trophic interactions within the nGoM. A total of 19 copepod feeding experiments were conducted using natural prey assemblages and the most common copepod grazers on cruises

during July/August of 2017, October 2017, January 2018 and March 2018. Changes in prey abundance and structure were assessed in response to the presence or absence of copepods using light microscopy. Copepod ingestion rates were calculated to compare overall intake and prey contributions to diet among onshore compared to offshore sites and among differing seasons.

The following hypotheses were tested:

H1: Copepod ingestion rates (IR) will differ with prey availability among on- to offshore sites and among seasons.

H2: Contributions from microzooplankton prey to copepod diets will increase from onshore to offshore and during low-productivity months as phytoplankton availability generally decreases.

H3: Microzooplankton standing stocks are top-down controlled at offshore sites, independent of season, and at nearshore stations during low-productivity months.

Material and Methods

Study Region and Feeding Experiments

A series of on-deck copepod grazing experiments were conducted along an on- to offshore transects during July/August 2017, October 2017, January 2018 and March 2018 (Fig. 1). The data for July/August 2017 was collected during a 5-week long NOAA-led Gulf of Mexico Ecosystems and Carbon Cruise (GOMECC-3) with a nearshore and offshore experiment at each of two transects; one off the Louisiana and the other off the Mexican coast (Fig. 1 and Table 1). The remaining three ~1-week cruises (NSF-funded RAPID initiative) all included a total of 5 experiments (3 onshore and 2 offshore locations) along 2 parallel transects off of Texas (Fig. 1 and Table 1). Along all transects several stops were made to obtain surface environmental data (5 – 10 m depth) using a CTD rosette including temperature (T in °C), salinity (S in psu), inorganic nutrients (µM for NO_2+NO_3, NH_4, PO_4, and SiO_4) and dissolved oxygen concentrations (DO in µg L^{-1}). From the same CTD casts, whole seawater (WSW) was collected, to obtain natural prey assemblages for the feeding experiments, and the WSW gently screened using a 200-µm Nitex mesh to remove mesozooplankton (exclusion treatment). Later analyses confirmed that the 200 µm mesh retained copepods, as well as most copepodites and nauplii, while only negligible numbers of large protists were caught on the mesh (mainly sarcodines and occasionally *Trichodesmium* colonies). For the copepod addition treatments, copepods were added to 1L bottles holding 200 µm-prescreened water (addition treatment). All bottles were incubated in triplicates for 24 hrs in an on-deck incubator at *in situ* temperature and 50% ambient light (Table 1). The only exception made to the size of the prescreen occurred for the onshore station TA_8 in March of 2018, where the tow overwhelmingly returned nauplii stages and our feeding experiment was adapted for this early life stage (Table 1). For this particular experiment, the

prescreening of the WSW and the removal of the nauplii at the end of the incubation was achieved using an 80 µm-mesh.

Copepods for addition experiments were collected using a 150-µm mesh zooplankton net in the upper water column (5 - 10 m; see further details below). Within ~1hr of the CTD cast, all treatment bottles were situated in the on-deck incubator. At the onset of each experiment (T_0) and at the final time point, prefiltered 200-µm seawater (150 - 350 mLs) was collected for chlorophyll *a* measurements (chl *a* in µg L^{-1}) and aliquots preserved using 5% acid-Lugol's solution to determine prey abundances, community structure and biovolumes (BV). A 200 µm-screen was also used to remove copepods from the addition bottles prior to the final time point. The metazoa were rinsed off the mesh with 0.2 µm-filtered seawater and preserved with Formalin (5% final concentration) for counting and sizing. All cruises combined, incubation temperatures varied from 11.9 °C in January 2018 to 28.4 °C in July of 2017 (Table 1). Each bottle had low concentrations of nitrogen and phosphate added (5 µM of N and 0.5 µM of P) to avoid nutrient limitation in bottles without copepod remineralizers (copepod exclusion treatments) (Landry et al. 1995)

Zooplankton Analyses and Copepod Collection

Copepods for the addition treatments were picked individually from each of the tows and rinsed using petri dishes filled with 0.2 µm-filtered seawater using a dissecting scope. After 2 - 3 rinses the same number of copepods were transferred into each of 3 addition treatment bottles (Table 1). Using a Folsom plankton splitter (Wildco), aliquots of the net-tow were also preserved for the characterization of the zooplankton community and to determine zooplankton displacement volumes (DV in ml per m^{-3}) (Wiebe et al. 1975). Contributions from major zooplankton groups were determined for multiple tow aliquots (8 – 25 mL) counted under a dissecting scope (at least

100 organisms) using a counting wheel (Wildco). Zooplankton DVs were normalized by tow volume and converted to particulate organic carbon (POC) using a previously established conversion factor of 21 mg C mL^{-1}, representative of a mixed zooplankton assemblage (Bode & Varela 1998).

Microplankton abundances, Community Structure, and Carbon Biomass

Protists in the 15 - 200 µm size fraction were enumerated by inverted light microscopy using standard settling techniques for samples (100 mL) preserved with Lugol's solution (5% final concentration) (Utermöhl 1958, Sherr et al. 1993). Protists were assigned to broad taxonomic groups based on morphological examination (diatoms, ciliates, and dinoflagellates) and assigned to genus and species level were possible. Cell biovolume (BV) was calculated from geometric shapes for 40–80 individual organisms for each protistan group (diatoms, dinoflagellates and ciliates) and for each of the 4 cruises. Average BVs were then converted into carbon (C) biomass (Table 6) by applying published conversion factors for ciliates with 0.19 pg C μm^{-3}, (Putt & Stoecker 1989), diatoms and dinoflagellates with pg C μm^{-3} = 0.288 $BV^{0.811}$ and pg C μm^{-3} = 0.76 $BV^{0.819}$, respectively (Menden-Deuer et al. 2000).

Chlorophyll *a* Measurements

For chl-*a* analyses, protistan biomass was concentrated onto a 25 mm Whatman GF/F and prior to measurements, pigments on the filters were extracted in acetone for 24 hours in -20C freezer. The extracted pigment was then measured on a TD10-AU fluorometer (Turner Designs) following previously published protocols (Parsons 2013).

Copepod Ingestion Rates

Daily copepod ingestion rates (IR) for diatoms, ciliates and dinoflagellates (in cells cop^{-1} d^{-1} or µg C cop^{-1} d^{-1}) were calculated from differences in the rates of change of prey abundance (or C biomass) among the treatments without copepods (exclusion treatment) compared to changes with copepods (addition treatment) (Frost 1972). Using a series of equations, prey growth in the absence of copepods was calculated first:

1) $$C_2 = C_1 \times e^{k\,(t2-t1)}$$

where k is the algal growth constant over the duration of the experiment (t2-t1), C_1 is the prey concentration at the beginning of the experiment and C_2 at the final time point. Next, the grazing constant (g) was determined using k and information on changes in prey concentration in the presence of copepod grazers (addition treatments):

2) $$C_2^* = C_1^* \times e^{(k-g)\,(t2-t1)}$$

where C_1^* and C_2^* are the cell (or C) concentrations in the addition treatments at time t1 and t2. The average cell concentration in each bottle <C> was then calculated for the same time interval where:

3) $$\langle C \rangle = \{C_1^* [e^{(k-g)\,(t2-t1)} - 1]\} / (k-g)\,(t2-t1)$$

Using the number of copepods (N) in each bottle and the incubation volume (V) allow for the calculation of filtration rates (F in ml cop^{-1} d^{-1}).

4) $$F = V\,g / N$$

Finally, both average prey concentrations <C> and filtration rate allow for the calculation of individual copepod ingestion rate (IR):

5) $$IR = \langle C \rangle \times F$$

IRs were calculated using changes in cell abundance (cells cop^{-1} d^{-1}) carbon biomass (µg C cop^{-1} d^{-1}). Decreases in biomass during the 24 hour incubations were assumed to be mainly the result of copepod predation (i.e. losses due to ciliates and heterotrophic dinoflagellates preying on each other were considered negligible).

Environmental Data

Physicochemical measurements were conducted on WSW samples collected from surface depth between 2 to 10 meters using a conductivity temperature depth (CTD) profiler equipped with 10-L Niskin bottles. Samples were taken to gather information on salinity, temperature, dissolved oxygen, and nutrients. The nutrients were analyzed at the Wetland Biogeochemistry Analytical Services Lab in Louisiana State University. Concentrations of NO_2+NO_3 were measured following EPA protocol 353.4, NH_4 levels were determined using EPA protocol 350.1, PO_4 concentrations via EPA protocol 365.5 and SiO_2 levels were determined using EPA protocol 366.0.

Statistical Analyses

Organismal abundance and/or taxa composition changes along spatial and temporal scales and shifts due to the exclusion treatments compared to grazer addition treatments were examined using multivariate analyses (PRIMER v7 statistics package (Anderson et al. 2008). Community data were square-root transformed and compared based on Bray–Curtis similarity indices. Physicochemical conditions were log-transformed, normalized (mean subtracted from each value and divided by the standard deviation) and compared after the computation of Euclidean distance resemblance matrices. IRs based on chl-*a*, cell abundance and C biomass were compared in the same manner to test for significant differences among different treatments with and without copepods. Negative IRs were replaced by zero values and the individual effects of copepod

presence (addition treatment) across seasons and locations tested via ANOSIM permutation analyses (Clarke & Warwick 2001). Temporal differences encompassed information from varying seasons including summer with July/ August 2017, fall with October 2017, winter with January 2018 and spring with March 2018. Spatial differences refer to distance from shore. This resulted in global *R* values as a measure of distinction between groups that indicated no difference among sites or treatments (R = 0 or low) or maximal group separation (R = 1 or high). Chl-*a* concentrations were examined for their relationships with physical (temperature, DO and pH) and chemical (NH_4, NO_3+NO_2, PO_4 and SiO_2) parameters using correlation and regression analyses (Pearson's product-moment correlations).

Results

Physicochemical Conditions

Comparisons among cruises showed seasonal differences for all parameters except for salinity and NH_4 concentrations (Table 2). These differences were strongest for surface temperature and PO_4 levels, followed by DO and chl-*a* concentrations (one-way ANOSIM; R = 0.212 – 0.591, P = 0.0001; Table 2). Only weak seasonality was indicated for NO_3+NO_2 and SiO_2 concentrations (one-way ANOSIM; R = 0.146 and 0.097, respectively; P < 0.05; Table 2). Average water temperatures were lowest with 19.0ºC in January 2018 and highest with 30.1ºC in July/August 2017 (Table 3 and 4). Over the four cruises, surface salinities and DO varied between 33.6 - 35.0 psu and from 4.4 - 5.0 mg L^{-1}, respectively (Table 3). On average, both parameters were at their lowest in July/August 2017 and at their highest in March 2018 (Table 4). Overall, inorganic nutrient concentrations ranged from 0 - 0.16 µM for NO_2+NO_3, 1.25 - 6.11 µM for NH_4, 0.10 - 0.33 µM PO_4, and 1.48 - 7.33 µM SiO_2 (Table 3). Average NO_2+NO_3 levels were highest during the July/August cruise in 2017, PO_4 and NH_4 concentrations in October 2017 and SiO_2 in January 2018 (Table 4).

Overall chl-*a* concentrations ranged from 0.01 to 3.20 µg L^{-1} across all seasons (mean = 0.46 µg L^{-1}; n = 39; Table 3). Correlation analyses indicated negative relationships of chl-*a* with temperature and salinity (r = -0.389 and -0.607, respectively; p < 0.05) and a positive relationship with DO (r = 0.400, p < 0.05, Table 5). On-to offshore differences for physicochemical parameters were also examined after grouping sampling sites based on their distance to shore with 0-50, 51-100, 100+ km off the coastline (Table 4). Salinity showed the strongest change with distance to shore, followed by DO, and SiO_2 levels (ANOSIM, *R* = 0.219 - 0.583, P = 0.0001 - 0.02; Table 2). Salinity increased with distance to shore while surface DO

concentrations decreased, but never fell below 4 mg L^{-1} except for a single observation in January 2018 at site TA4, when a minimum of 2.8 mg L^{-1} was detected. SiO_2 followed the same trend as DO and decreased from ~ 6.7 µM to 2 – 3 µM from within 50 km nearshore to further offshore (Table 4). Combining all site-specific physicochemical parameters to compare environmental "fingerprints" within and among seasons and across locations indicated that season and distance to shore were equally strong drivers of environmental conditions (R = 0.592 and 0.655, respectively, P = 0.0001; two-way crossed ANOSIM). Additional, historical chl-*a* data for the Texas transect was also available through the Southeast Area Monitoring and Assessment Program (SEAMAP). Chl-*a* data collection through SEAMAP had mainly been limited to spring and fall and ten-year averages for this data show that chl-*a* concentrations tend to be consistently higher over the shelf (onshore) compared to the stations above the continental slope (offshore). Moreover, seasonal differences in phytoplankton biomass are apparent close to shore but not when spring and fall data were compared out on the continental slope (Kurtay and Stauffer, in preparation).

Per Cell Carbon Content of Microplankton

Community analyses, standing stock estimates and feeding experiments were conducted for five onshore sites that were located within the 0 – 50 km distance range (TB1, TA2, TB3, L1, and M1) which corresponded to water column depths of < 50 m (Table 2). All offshore stations were located at least 100 km from shore (L3, M3, TA8, and TB9) and corresponded to depths of > 1,000 m (Table 2). To determine C prey stocks, C cell contents were calculated from biovolume estimates (not shown) for the entire microplankton community, as well as the three major prey groups. Overall, C content per cell for ciliates ranged from 227 – 4,352 pg C $cell^{-1}$ (mean = 1,566 pg C $cell^{-1}$; n = 19), for diatoms from 113 – 2,412 pg C $cell^{-1}$ (mean = 1,267 pg C $cell^{-1}$; n = 19)

and for dinoflagellates from 440 – 2,790 pg C cell^{-1} (mean = 1,093 pg C cell^{-1}; n = 19; Table 6 and Figure 2). These values corresponded to overall mean values of 1,566 pg C µm^{-3} for ciliates, 1,267 pg C µm^{-3} for diatoms and 1,093 pg C µm^{-3} for dinoflagellates. No differences were observed in cell C for prey groups when compared across seasons or with distance to shore ($P > 0.05$), most likely due to considerable variability within and among the prey types (Figure 2).

Initial Microplankton Biomass and Community Structure

Total initial prey biomass was calculated from cell C content estimates and using abundances at the onset of each experiment. Overall, these values ranged from 1.2 - 13,853 µg C L^{-1} (mean = 1,576 µg C L^{-1}; n = 19; Table 7) for all groups combined with no difference across seasons ($P > 0.05$). Prey biomass estimates did vary with distance to shore ($R = 0.297$ at $P = 0.0006$; one -way ANOSIM), with maxima close to shore (range = 48 -13,853 µg C L^{-1} for 0 – 50 km range; n = 11) and decreases offshore (range = 1.2 – 256 µg C L^{-1} for 100+ km; n = 8; Table 7 and Figure 3).

Initial microplankton community structure based on microscopy analyses allowed for the identification of a total of 43 genera/major groups (Table 8) and varied with season ($R = 0.333$ at $P = 0.006$) and even more strongly with distance to shore ($R = 0.564$ at $P = 0.009$; two-way crossed ANOSIM). Diatom taxa were dominant members of onshore assemblages (0 – 50 km) contributing an average of ~75% to total C (Figure 4) compared to ~27% C at offshore sites. The dominant diatom genera included *Skeletonema* spp., *Chaetoceros* spp., and *Leptocylindrus* spp.. In contrast to the diatoms, ciliates and dinoflagellates made up ~11% and 13% of total C onshore and 30% and 43% offshore, respectively (Table 8 and Figure 4). *Gymnodinium* and *Gyrodinium* spp. dominated the dinoflagellate assemblage and members of the genus *Strombidium* were the most common ciliates.

Zooplankton Biomass and Community Structure

Zooplankton C biomass estimates were based on DVs and ranged from 1.7 - 7.6 µg C L^{-1} (mean = 4.3, n = 19; Table 9). Comparisons showed that overall C biomass did not differ with season or distance to shore ($P > 0.05$). Zooplankton community structure varied with season ($R = 0.270$ at $P = 0.004$) but not with distance to shore. Major taxonomic groups included copepods, other crustaceans (cladocerans, euphausiids, and others), cnidarians, chaetognaths, molluscs, tunicates (mainly larvaceans), polychaets, and invertebrate larvae (Table 10 and Figure 5). Numerically, copepods made up between 18 to 94% of the assemblage (mean = 52%; n=19) with maximum levels observed for the Louisiana transect in July 2017 (see L1 in Table 10 and Figure 5). Larvaceans contributed strongly to onshore communities, especially in October 2017, where they made up ~44% of the zooplankton counts. Overall, larvaceans contributed ~23% to onshore and 16% to the offshore communities (Table 10). Not included in these estimates were fish eggs and sarcodines (mainly acantharia) that were occasionally observed at high numbers in the tows (Table 10). Fish eggs were mostly encountered at onshore sites while acantharia were found all across stations and seasons (Table 10). *Trichodesmium* colonies were seen in high abundances offshore in July/August 2017 (Table 10).

Copepod Ingestion Rates and Prey Community Shifts

Copepod IRs were derived using differences in chl-*a* (µg chl-*a* cop^{-1} day^{-1}), cell abundance (cells cop^{-1} d^{-1}), and C biomass (µg C cop^{-1} d^{-1}) between exclusion and copepod addition treatments. Negative IRs indicated no measurable effect of copepod feeding on chl-*a* concentrations (or prey abundance) and/or the increase of chl-*a* concentrations (or prey abundance) due to growth exceeding removal by copepod consumers over the duration of the feeding experiments (Frost 1972). IRs ranged from 0 - 11 µg Chl-*a* cop^{-1} d^{-1} (mean = 1.36 µg Chl-*a* cop^{-1} d^{-1}; n = 17; Table

11A). No apparent trends could be discerned based on pigment estimates across seasons or locations ($P > 0.05$; Table 12). Abundance-based total IRs ranged from 37 - 15,922 cells cop d^{-1} (mean = 2.302 cells cop d^{-1}; n = 17; Table 11A). Comparison for the differing prey types showed that average IRs where highest and most variable for copepods consuming dinoflagellates (1,049 ± 2,722 cells cop d^{-1}), followed by diatoms (1,316 ± 1,791 cells cop $d^{-1)}$ and ciliates (415 ± 494 cells cop d^{-1}, Table 11A).

Total C-based IRs (all microplankton combined) ranged from 0.01 to 194.24 µg C cop^{-1} d^{-1} (mean = 47.43; n = 19, Table 11B). Comparing total and prey-specific C IRs across season showed that they varied slightly with the exception of dinoflagellate prey ($R = 0.047$ - 0.192; P = 0.03 – 0.001; one-way ANOSIM; Table 13). For both ciliates and diatoms, IRs were lowest during July/August 2017 and some of the highest rates observed during October 2017 and/or January 2018 (Table 13). Additionally, average IRs tended to be higher onshore for the different taxa and total C (Table 12). Spatial variations were only seen for dinoflagellate consumption and total C IR ($R = 0.067 – 0.091$ at $P < 0.05$; one-way ANOSIM; Table 13). Overall, dinoflagellate consumption by copepods was higher offshore and reached a maximum of 122.67 µg C cop^{-1} d^{-1} at site TA2 in January 2018 (Table 11B and Figure 6). C IR for ciliate and diatom prey tended to be higher at onshore sites (there was no significant difference at $P > 0.05$) with an overall maximum of 84.58 µg C cop^{-1} d^{-1} and 207.40 µg C cop^{-1} d^{-1}, respectively (Table 11B and Figure 6).

Changes in the relative prey contributions did not vary over seasons or distance to shore ($P > 0.5$). Contributions from diatom biomass to copepod diet were matched by contributions from heterotrophic/mixotrophic prey (ciliates and dinoflagellates) in several of the experiments (Figure 7). In summer (July/August 2017), when IRs were generally low (Figure 7),

dinoflagellates played an important role in copepod diets followed by diatoms, whereas ciliates were almost entirely absent from copepod diets (relative contributions <1%) along the M and L transects (Figure 7). This seemed in contrast to observations from other cruise events where ciliates made considerable contributions to prey intake, especially offshore (TA8 and TA 9, Figure 16). Ciliate intake also exceeded diatom C consumption at onshore stations TB1 in October 2017 and TB3 in January 2018, (Table 16). Overall, diet composition varied considerably over seasons and distance to shore but increases in prey-specific IRs were correlated with prey concentrations (Figure 8). Independent of prey type, copepod feeding seemed to approach maximum IRs (Figure 8). Average contributions from diatom prey to copepod diet ranged from 31 to 52%, from ciliate prey between < 1 and 44% and for dinoflagellate biomass from 15 to 48% (Table 16). Examining the effect of copepod additions (presence versus absence) on final prey community composition revealed that the initial differences in prey assemblages (e.g., based on distance to shore), had a much stronger impact on prey communities than predator presence/absence (two-way crossed ANOSIM, Table 14). Indeed, prey community structure was only significantly impacted by copepod grazing activity during the October cruise (R = 0.211; p = 0.006; n = 15; Table 14).

Copepod Grazing Impact on Prey Standing Stocks

Copepod abundances within the treatment bottles corresponded well with natural copepod densities based on zooplankton tow estimates (mean for addition treatments = 15 cop L^{-1}; range = 8 - 21 cop L^{-1}, Table 15). Employing individual copepod IRs from the experiments, overall C ingestion for the entire copepod assemblage was calculated (µg C cop assemblage d^{-1}) and the estimates compared to prey biomass to examine the potential impact of copepod feeding on prey standing stocks (Table 15). The amount of microplankton standing stocks removed by copepod

feeding was higher offshore than at the nearshore sites (*R*= 0.183; P=0.027, one-way ANOSIM; Table 15), but no trends were detected across seasons (P> 0.05). Overall, ciliate ingestion by copepod grazers resulted in the removal of ~34% of the standing stock ranging from 0.13 to 49.9 % and the highest estimates were derived during October 2017 offshore with 70% (Table 15). Ciliates standing stock like the overall, varied over distance to shore (*R*= 0.201; P= 0.027, one-way ANOSIM; Table 15). On average, ~26% (range = 22 -31%) and 52% (range = 16 – 134%) of diatom and dinoflagellate standing stocks were consumed, respectively. Diatoms standing stock varied over distance to shore same as the diatoms (*R*= 0.384; P= 0.004, one-way ANOSIM; Table 15) but not seasonally. Dinoflagellate abundances did vary spatially or seasonally (P> 0.5). Maximum removal estimates were obtained for March 2018 for diatoms and in July/ August 2017 for dinoflagellates.

Discussion

Copepod Grazing and Diet Composition

Relative contributions from heterotrophic/mixotrophic dinoflagellates and ciliates to copepod diet in the nGOM exceeded C intake from diatoms in 15 out of 19 experiments (mean = 69%; overall range = < 1 – 100%; Figure 7). This was most pronounced for offshore stations (TA8 and TB9), where diatoms were a less abundant food source but was also observed onshore in summer 2017 (L and M transects) and in March 2018 (TA2 and TB3; Figure 6). These findings further support that the traditional view of copepods as being mainly herbivorous and sustaining themselves grazing on primary producers such as diatoms is too simplistic for models of energy flow and biogeochemical cycling at the base of food webs (Steinberg & Landry 2017, Turner et. al. 2001, Stoecker & Capuzzo, 1990). In the nGOM, copepod IRs as well as diet composition differed strongly between nearshore (water column depth < 50 m) where there was higher prey biomass (>250 μg C L^{-1}), compared to offshore (water column depth > 1,000 m) with less prey availability (<50 μg C L^{-1}) but was hardly related to season. Since maximum nearshore chl-*a* concentrations during the March 2018 cruise averaged only 1.6 μg L^{-1} (range from < 1 to 3.02 μg L^{-1}, Table 4) the assumption was made that this study did not capture the conditions that characterize the productive spring season in the nGOM. Previously, average chl-*a* levels of 7.5 to 8.5 μg L^{-1} have been reported for spring season along the inner shelf while levels of ≤ 0.5 μg L^{-1} seem characteristic for offshore waters year-round (Chakraborty & Lohrenz 2015, Mendelssohn et al. 2017).

A review on copepod feeding that examined prey contributions to the diet in relation to ecosystem productivity showed that the median for ciliate C contributions falls around ~32% C in eutrophic systems compared to ~15% in oligotrophic systems (Saiz & Calbet 2011). In good

agreement - and considering the predominantly oligotrophic conditions that prevailed during the cruise efforts in this study - median ciliate contributions to the copepod's diet amounted to ~16% and those from dinoflagellates to ~19% (Fig 7). Comparing IR estimates across all experiments showed C consumption kept increasing with prey concentrations (C) independent of prey type and that copepods did not reach maxim IR under natural prey densities (Figure 8). With an overall average for copepod IRs of 47 µg C cop^{-1} d^{-1} and a maximum of 194 µg C cop^{-1} d^{-1} (all prey groups combined), these values fell within the upper range of previously reported field IRs (see review in Saiz and Calbet, 2011). Consistent with findings from other field studies, food limitation seemed to constrain copepod feeding in the nGOM (Saiz & Calbet 2007).

Copepod Grazing Impact on Microplankton Assemblages

The impact of copepod grazing on microplankton biomass varied markedly across all experiments and copepod feeding impacted prey standing stocks differently at the onshore versus offshore sites, while seasons did not seem to make a difference for biomass removal (Table 15B). Ciliates and diatoms tended to experience higher grazing pressure at nearshore sites, and dinoflagellate populations were more strongly impacted at offshore sites (Table 15B). Overall, ranges for average daily removal of prey stocks spanned from <1% to 134% (mean = 38%). It is important to note that these estimates are approximations that depend greatly on the accuracy of determining prey and predator abundances. Typically, as in this study, such abundances were based on a limited number of observations (e.g., zooplankton tows, CTD casts) that do not take into account spatial or temporal patchiness in prey and predator distribution. This spatial patchiness likely contributed to maximum removal estimates that exceeded 100% of the resident microplankton population. In a single case, this resulted in a removal estimate of ~500% (L1 in July/August 2017) and was linked to copepod abundances that exceeded those from all other

locations by 1-2 orders of magnitude (454 cop m^{-3}, Table 10). Overall, mesozooplankton densities in this study matched well with previously reported values for the nGOM (Elliott et al. 2012, Kimmel et al. 2009, Mendelssohn et al. 2017).

Examining protistan community structure at the genus level, rather than looking at shifts in the three major prey groups, further highlighted the strong differences between on-and offshore trophic dynamics, while there was no consistent trend across seasons (Table 14). Somewhat surprisingly, significant differences in final microplankton community structure associated with copepod absence/presence (comparing exclusion and addition treatments) were only observable in October 2017. We hypothesize that this indicates that microplankton community composition was already constrained by top-down processes when experiments were conducted during the other seasons. Our study emphasizes the importance of resolving microplankton-copepod dynamics across spatial and temporal scales. Traditionally, the ecological roles of mesozooplankton grazers (i.e., copepods) has often been represented simplistically in biogeochemical models but subtle changes in IR and food selection drive both C cycling and export within the ocean. Providing new data on spatiotemporal patterns for copepod feeding in the nGOM can serve as a model for other marine environments as we aim to understand the impact of eutrophication on plankton food webs (Rabalais et al. 2002, Justić et al. 2005)

REFERENCES

Benedetti F, Gasparini S, Ayata S-D (2015) Identifying copepod functional groups from species functional traits. Journal of Plankton Research 38:159-166

Berggreen U, Hansen B, Kiørboe T (1988) Food size spectra, ingestion and growth of the copepod *Acartia tonsa* during development: Implications for determination of copepod production. Marine biology 99:341-352

Blaxter JH, Douglas B, Tyler PA, Mauchline J (1998) The biology of calanoid copepods, Vol 33. Academic Press

Bode A, Varela M (1998) Primary production and phytoplankton in three Galician Rias Altas (NW Spain): seasonal and spatial variability. Scientia Marina 62:319-330

Broglio E, Saiz E, Calbet A, Trepat I, Alcaraz M (2004) Trophic impact and prey selection by crustacean zooplankton on the microbial communities of an oligotrophic coastal area (NW Mediterranean Sea). Aquatic Microbial Ecology 35:65-78

Calbet A (2001) Mesozooplankton grazing effect on primary production: a global comparative analysis in marine ecosystems. Limnology and Oceanography 46:1824-1830

Calbet A (2008) The trophic roles of microzooplankton in marine systems. ICES Journal of Marine Science 65:325-331

Calbet A, Landry MRJL, Oceanography (2004) Phytoplankton growth, microzooplankton grazing, and carbon cycling in marine systems. 49:51-57

Chakraborty S, Lohrenz SE (2015) Phytoplankton community structure in the river-influenced continental margin of the northern Gulf of Mexico. Marine Ecology Progress Series 521:31-47

Elliott DT, Pierson JJ, Roman MR (2012) Relationship between environmental conditions and zooplankton community structure during summer hypoxia in the northern Gulf of Mexico. Journal of plankton research 34:602-613

Fessenden L, Cowles TJ (1994) Copepod predation on phagotrophic ciliates in Oregon coastal waters. Marine Ecology-Progress Series 107:103-103

Frost BW (1972) Effects of size and concentration of food particles on the feeding behavior of the marine planktonic copepod *calanus pacificus*1. 17:805-815

Hansen B, Bjornsen PK, Hansen PJJL, oceanography (1994) The size ratio between planktonic predators and their prey. 39:395-403

Justić D, Rabalais NN, Turner RE (2005) Coupling between climate variability and coastal eutrophication: evidence and outlook for the northern Gulf of Mexico. Journal of Sea Research 54:25-35

Kimmel DG, Boicourt WC, Pierson JJ, Roman MR, Zhang XJJoEMB, Ecology (2009) A comparison of the mesozooplankton response to hypoxia in Chesapeake Bay and the northern Gulf of Mexico using the biomass size spectrum. 381:S65-S73

Kleppel G, Pieper R, Trager G (1988) Variability in the gut contents of individual *Acartia tonsa* from waters off Southern California. Marine Biology 97:185-190

Kleppel GJME-PS (1993) On the diets of calanoid copepods. 99:183-183

Landry M, Kirshtein J, Constantinou J (1995) A refined dilution technique for measuring the community grazing impact of microzooplankton, with experimental tests in the central equatorial Pacific. Marine ecology progress series Oldendorf 120:53-63

Lichti DA, Rinchard J, Kimmel DG (2017) Changes in zooplankton community, and seston and zooplankton fatty acid profiles at the freshwater/saltwater interface of the Chowan River, North Carolina. PeerJ 5:e3667

López E, Anadón R (2008) Copepod communities along an Atlantic Meridional Transect: Abundance, size structure, and grazing rates. Deep Sea Research Part I: Oceanographic Research Papers 55:1375-1391

Mendelssohn IA, Byrnes MR, Kneib RT, Vittor BA (2017) Coastal Habitats of the Gulf of Mexico. In: Ward CH (ed) Habitats and Biota of the Gulf of Mexico: Before the Deepwater Horizon Oil Spill: Volume 1: Water Quality, Sediments, Sediment Contaminants, Oil and Gas Seeps, Coastal Habitats, Offshore Plankton and Benthos, and Shellfish. Springer New York, New York, NY

Menden-Deuer S, Lessard EJJL, oceanography (2000) Carbon to volume relationships for dinoflagellates, diatoms, and other protist plankton. 45:569-579

Parsons TR (2013) A manual of chemical & biological methods for seawater analysis. Elsevier

Putt M, Stoecker DK (1989) An experimentally determined carbon: volume ratio for marine “oligotrichous” ciliates from estuarine and coastal waters. Limnology and Oceanography 34:1097-1103

Rabalais NN, Turner RE, Wiseman Jr WJ (2002) Gulf of Mexico hypoxia, aka “The dead zone”. Annual Review of ecology and Systematics 33:235-263

Saiz E, Calbet A (2007) Scaling of feeding in marine calanoid copepods. Limnology and Oceanography 52:668-675

Saiz E, Calbet A (2011) Copepod feeding in the ocean: scaling patterns, composition of their diet and the bias of estimates due to microzooplankton grazing during incubations. Hydrobiologia 666:181-196

Schnetzer A, Caron DA (2005) Copepod grazing impact on the trophic structure of the microbial assemblage of the San Pedro Channel, California. Journal of Plankton Research 27:959-971

Schnetzer A, Steinberg D (2002) Natural diets of vertically migrating zooplankton in the Sargasso Sea. Marine Biology 141:89-99

Sherr EB, Caron DA, Sherr BF (1993) Staining of heterotrophic protists for visualization via epifluorescence microscopy. Handbook of methods in aquatic microbial ecology:213-227

Sherr EB, Sherr BF (2007) Heterotrophic dinoflagellates: a significant component of microzooplankton biomass and major grazers of diatoms in the sea. Marine Ecology Progress Series 352:187-197

Steinberg DK, Landry MR (2017) Zooplankton and the Ocean Carbon Cycle. 9:413-444

Stoecker DK, Capuzzo JMJJoPR (1990) Predation on protozoa: its importance to zooplankton. 12:891-908

Troedsson C, Simonelli P, Nägele V, Nejstgaard JC, Frischer ME (2009) Quantification of copepod gut content by differential length amplification quantitative PCR (dla-qPCR). Marine Biology 156:253-259

Turner JT (2004) The importance of small planktonic copepods and their roles in pelagic marine food webs. 43:255-266

Turner JT, Levinsen H, Nielsen TG, Hansen BW (2001) Zooplankton feeding ecology: grazing on phytoplankton and predation on protozoans by copepod and barnacle nauplii in Disko Bay, West Greenland. Marine Ecology Progress Series 221:209-219

Utermöhl HJIVftuaLM (1958) Zur Vervollkommnung der quantitativen Phytoplankton-Methodik: Mit 1 Tabelle und 15 abbildungen im Text und auf 1 Tafel. 9:1-38

Wiebe PH, Boyd S, Cox JL (1975) Relationships between Zooplankton Displacement Volume, Wet Weight, Dry Weight, and Carbon. Fishery Bulletin 73:777-786

Table 1: Sampling site information and experimental details listing the months, transects, individual station numbers and coordinates for each location (see also Fig. 1). Also shown are the dates when the experiments were conducted together with incubation temperatures (°C), duration (hrs), and the average number of copepods (cop L^{-1}) added to triplicate addition treatment bottles with their standard deviations (SD). L = Louisiana transect; M = Mexico transect, TA and TB = Texas transects A and B; * denotes nauplii

	Exp Locations		Coordinates		Dates	Temp	IncubTime	Cop L^{-1}
	Transect	Site ID	Lat N	Long W		°C	hrs	Ave
July/August 2017	L	1	28.87	90.47	7/27/2017	28.4	21	21
	L	3	27.58	90.00	7/26/2017	28.4	24	18
	M	1	25.88	96.82	8/2/2017	24.2	22	10
	M	3	25.88	94.67	8/3/2017	26.3	24	12
October 2017	TB	1	29.30	94.40	11/2/2017	22.9	21	15
	TA	2	29.00	95.00	10/29/2017	23.1	24	12
	TB	3	29.00	94.50	11/1/2017	23.6	20	20
	TA	8	27.33	95.00	10/30/2017	26.9	23	9
	TB	9	27.32	94.46	10/31/2017	27.3	25	15
January 2018	TB	1	29.30	94.40	1/12/2018	11.9	23	11
	TA	2	29.00	95.00	1/11/2018	12.1	23	9
	TB	3	29.00	94.50	1/11/2018	15.4	20	17
	TA	8	27.33	95.00	1/9/2018	22.9	24	9
	TB	9	27.32	94.46	1/9/2018	23.4	25	8
March 2018	TB	1	29.30	94.40	3/19/2018	19.6	19	20
	TA	2	29.00	95.00	3/20/2018	20.5	23	20
	TB	3	29.00	94.50	3/19/2018	19.5	24	20
	TA	8	27.33	95.00	3/21/2018	22.4	24	15*
	TB	9	27.32	94.46	3/21/2018	22.3	24	15

Table 2: Results of one-way ANOSIM comparing individual environmental factors across four seasons and for site location/distance to shore (0 – 50, 51 – 100 and 100+ km). All global tests were run at 9999 permutations. P = significance level; NS = not significant at $P < 0.05$. Note: *R* values typically range from 0 to 1, where *R* equal to 0 indicates that the physicochemical measures are not dissimilar among sample groups (i.e., seasons or distance to shore), whereas *R* equal to 1 indicates strong dissimilarities among sample groups.

	Season		**Distance**	
	R	P	*R*	P
Temp	0.591	0.0001		NS
chl *a*	0.212	0.0001	0.244	0.005
Sal		NS	0.583	0.0001
DO	0.298	0.0001	0.236	0.02
NO_2+NO_3	0.146	0.0005		NS
NH_4		NS		NS
PO_4	0.457	0.0001		NS
SiO_2	0.097	0.016	0.219	0.005

Table 3: Physicochemical data from sampling transects including temperature (°C), salinity (psu), nutrients (µM NO_2+NO_3, NH_4, PO_4, and SiO_4) and chl-*a* (µg L^{-1}). Note: values for all stations that were sampled along each transect are included, not only those locations where feeding experiments were conducted (see also Fig. 1). Also listed are overall water column depths (m) and the shortest distance to shore from each site (km).

	Transect	Site ID	Depth m	Distance to Shore km	Chl *a* µg L^{-1}	Temp °C	Sal	DO mg L^{-1}	NO_2+NO_3 µM	NH_4 µM	PO_4 µM	SiO_2 µM
July/August 2017	L	1	18	34	0.81	30.06	25.90	4.35	0.10	-	0.11	12.50
	L	2	47	43	1.39	30.27	27.71	4.63	0.10	-	0.17	13.70
	L	3	1257	168	0.05	30.69	35.98	4.35	0.70	-	0.00	1.90
	TA	2	16	19	0.06	30.21	34.42	4.55	0.10	-	0.26	11.20
	TA	6	62	120	0.77	29.68	36.22	4.31	0.40	-	0.07	1.90
	TA	10	537	224	0.07	30.80	32.93	4.33	0.02	-	0.05	3.10
	M	1	43	33	0.01	28.64	36.04	4.41	0.00	-	0.06	2.90
	M	2	792	107	0.01	30.11	36.48	4.35	0.00	-	0.06	0.30
	M	3	3185	148	0.08	30.17	36.51	4.33	0.10	-	0.08	1.60
		Ave	662	99	0.36	30.07	33.58	4.40	0.17	-	0.10	5.46
		SD	1043	72	0.50	0.63	4.04	0.11	0.23	-	0.08	5.35
October 2017	TB	1	14	25	0.26	22.88	30.48	5.04	0.00	6.84	0.35	10.50
	TA	2	16	19	0.44	23.07	32.77	4.74	0.00	5.76	0.37	4.92
	TB	3	18	50	0.32	23.56	32.42	4.95	0.00	6.12	0.33	3.49
	TA	4	34	74	0.62	23.74	33.13	4.90	0.03	5.11	0.36	3.83
	TB	5	37	112	0.28	24.55	35.00	4.68	0.00	6.62	0.34	4.19
	TA	6	62	120	0.40	26.38	36.24	4.37	0.03	4.78	0.34	3.08
	TB	7	73	167	0.15	26.04	36.14	4.47	0.00	5.19	0.30	1.48
	TA	8	1108	203	0.14	26.95	36.32	4.48	0.00	6.27	0.34	1.29
	TB	9	1259	240	0.12	27.3	36.29	4.47	0.00	5.11	0.33	2.26
	TA	10	537	224	0.10	26.92	36.36	4.38	0.00	9.27	0.31	1.03
		Ave	316	123	0.28	25.14	34.52	4.65	0.01	6.11	0.34	3.61
		SD	485	82	0.17	1.75	2.14	0.25	0.01	1.31	0.02	2.75
January 2018	TB	1	14	25	3.08	11.91	30.61	5.97	-	-	-	-
	TA	2	16	19	1.00	12.12	30.84	6.05	0.00	6.64	0.28	10.30
	TB	3	18	50	0.41	15.38	34.26	5.55	0.13	5.11	0.33	3.94
	TA	4	34	74	0.31	18.8	36.09	2.78	0.00	4.24	0.35	1.56
	TB	5	37	112	0.29	19.73	36.16	5.04	0.00	6.45	0.31	1.64
	TA	6	62	120	0.35	20.28	35.99	4.93	0.11	7.36	0.30	37.14
	TB	7	73	167	0.35	22.48	36.25	4.72	0.00	5.65	0.32	4.25
	TA	8	1108	203	0.37	22.9	36.28	4.65	0.00	4.86	0.32	1.88
	TB	9	1259	240	0.41	23.41	36.33	4.62	0.00	4.62	0.31	1.12
	TA	10	537	224	0.31	22.77	36.18	4.63	0.03	8.65	0.32	4.17
		Ave	316	123	0.69	18.98	34.90	4.89	0.03	5.95	0.32	7.33
		SD	485	82	0.87	4.40	2.28	0.92	0.05	1.44	0.02	11.52
March 2018	TB	1	14	25	3.20	19.56	31.04	4.94	0.00	1.85	0.20	2.86
	TA	2	16	19	1.39	20.54	29.92	5.32	0.00	0.41	0.33	2.21
	TB	3	18	50	0.10	19.46	34.96	5.06	0.00	1.49	0.33	1.52
	TA	4	34	74	0.11	21.3	36.25	4.88	0.00	2.25	0.22	0.83
	TB	5	37	112	0.10	21.05	36.35	4.91	0.00	1.00	0.27	1.44
	TA	6	62	120	0.08	20.55	36.16	4.98	0.00	0.49	0.28	1.30
	TB	7	73	167	0.04	21.05	36.26	4.93	0.00	1.93	0.27	1.05
	TA	8	1108	203	0.08	22.36	36.45	4.75	0.00	0.86	0.27	1.15
	TB	9	1259	240	0.03	22.34	36.49	4.79	0.00	0.22	0.27	1.31
	TA	10	537	224	0.03	22.39	36.55	4.75	0.00	1.99	0.29	1.11
		Ave	316	123	0.52	21.06	35.04	4.93	0.00	1.25	0.27	1.48
		SD	485	82	1.03	1.08	2.46	0.17	0.00	0.74	0.04	0.61

Table 4: Average values (Ave) with their standard deviation (SD) for physical and chemical factors grouped by season and by location (distance to shore). N = total number of observations for average calculations

Seasons	**N**	**Chl-*a* (µg L^{-1})**		**Temp (°C)**		**Sal (psu)**		**DO (mg L^{-1})**		**NO_2+NO_3 (µM)**		**NH_4 (µM)**		**PO_4 (µM)**		**SiO_2 (µM)**	
		Ave	SD	Ave	SD	Ave	SD	Ave	SD	Ave	SD	Ave	SD	Ave	SD	Ave	SD
July/August 2017	9	0.36	0.50	30.07	0.63	33.58	4.04	4.40	0.11	0.17	0.23	-	-	0.10	0.08	5.46	5.35
October 2017	10	0.28	0.17	25.14	1.75	34.52	2.14	4.65	0.25	0.01	0.01	6.11	1.31	0.34	0.02	3.61	2.75
January 2018	10	0.69	0.87	18.98	4.40	34.90	2.28	4.89	0.92	0.03	0.05	5.95	1.44	0.32	0.02	7.33	11.52
March 2018	10	0.52	1.03	21.06	1.08	35.04	2.46	4.93	0.17	0.00	0.00	1.25	0.74	0.27	0.04	1.48	0.61
Distance to Shore (km)	**N**																
0 - 50	13	0.96	1.07	22.13	6.50	31.64	2.91	5.04	0.55	0.04	0.05	4.28	2.59	0.26	0.10	6.67	4.55
51 - 100	3	0.34	0.26	21.28	2.47	35.16	1.76	4.19	1.22	0.01	0.02	3.87	1.47	0.31	0.08	2.07	1.56
100+	23	0.20	0.18	24.82	3.67	36.08	0.75	4.62	0.24	0.06	0.16	4.52	2.82	0.25	0.11	3.46	7.42

Table 5: Results from correlation analyses. Pearson's correlation coefficients (r) shown in bold are significant at $p < 0.05$ (df = 37). Chl-*a* = chlorophyll a; Temp = temperature; DO = dissolved oxygen

	Chl *a*
Temp	**-0.389**
Sal	**-0.607**
DO	**0.400**
NO_2+NO_3	-0.008
NH_4	-0.120
PO_4	-0.079
SiO_2	0.146

Table 6: Major microplankton taxa identified to genus or, where possible, species level using microscopy.

Major Taxa	Group	Genus / Species
Ciliates	Heterotroph	*Strombidium*
		unidentified tintinnids
	Mixotroph	*Laboea strobila*
		Myrionecta rubrum
Dinoflagellates	Photo/mixotrophs	*Prorocentrum*
		Ceratium
		Gymnodinium
		Gymnodinioids
		Scrippsiella
		Oxytoxum
	Heterotrophs	*Protoperidinium*
		Gyrodinium
Diatoms	Pennates	*Asterionellopsis*
		Thalassionema
		Nitzschia
		Cylindrotheca
		Pseudo-nitzschia
		Pleurosigma
		Navicula
		Entomoneis
		Licmorpha
		Bacillaria
		unidentified pennates
	Centric	*Thalassiosira*
		Cerataulina
		Coscinodiscus
		Leptocylindrus
		Chaetoceros
		Rhizosolenia
		Ditylum
		Odontella
		Guinardia
		Melosira
		Corethron
		Skeletonema
		Bacteriastrum
		Hemiaulus
		unidentified centrics
Ochrophytes		*Mallomonas*
Silicoflagellate		*Dictyocha*
Haptophytes		unidentified coccholithophorids
Sarcodines		unidentified radiolarians
		unidentified acanthatrians

Table 7: Average cell carbon content for diatoms, ciliates and dinoflagellates in initial seawater samples (pg C cell^{-1}) for each cruise period shown with their standard deviation (±SD).

	Transect	Site ID	Diatoms pg C cell^{-1}			Ciliates pg C cell^{-1}			Dinoflagellates pg C cell^{-1}		
			Ave	± SD	n	Ave	± SD	n	Ave	± SD	n
July/August 2017	L	1	1,176	1,434	9	227	12	2	536	404	14
	L	3	1,177	870	9	1,373	2,311	11	1,727	4,355	26
	M	1	853	727	15	2,677	3,125	6	1,109	1,067	17
	M	3	1,831	3,038	8	498	0	1	908	649	22
		Ave	1,185	1,517	41	1,781	1,362	20	1,153	1,619	79
October 2017	TB	1	1,458	2,114	22	4,352	7,949	11	1,316	1,049	23
	TA	2	1,563	3,586	26	818	204	2	2,790	2,619	6
	TB	3	781	2,014	24	2,055	1,487	5	1,933	2,622	17
	TA	8	1,915	2,573	5	1,425	2,032	11	1,288	1,816	22
	TB	9	1,409	1,686	9	1,164	1,263	10	620	1,054	18
		Ave	1,322	2,394	64	2,233	2,587	28	1,388	1,832	63
January 2018	TB	1	1,717	2,432	29	1,533	1,121	11	588	615	21
	TA	2	1,458	1,939	33	2,048	1,619	7	440	169	17
	TB	3	1,260	1,741	21	4,250	2,492	5	738	953	16
	TA	8	1,112	1,867	21	1,311	1,926	13	1,042	1,031	14
	TB	9	779	1,416	23	1,237	1,528	11	534	546	20
		Ave	1,304	1,879	98	1,696	1,737	36	647	663	67
March 2018	TB	1	2,412	5,198	37	537	255	10	539	725	22
	TA	2	1,540	1,866	29	1,102	168	2	2,240	2,876	9
	TB	3	1,276	1,547	16	1,450	1,095	7	947	961	25
	TA	8	250	202	2	810	649	7	851	1,461	20
	TB	9	113	74	11	884	867	11	630	711	25
		Ave	1,643	1,778	58	895	607	27	876	1,347	79

Table 8: Carbon biomass (µg C L^{-1}) in initial seawater sample during each of the seasons and individual stations.

	Exp Locations		**Diatoms**	**Ciliates**	**Dinoflagellates**
	Transect	**Site ID**	µg C L^{-1}	µg C L^{-1}	µg C L^{-1}
July/August 2017	L	1	187	1	14
	L	3	19	22	129
	M	1	19	0	29
	M	3	0	0	1
October 2017	TB	1	613	549	267
	TA	2	2,303	45	261
	TB	3	670	298	312
	TA	8	14	28	62
	TB	9	19	34	15
January 2018	TB	1	1,579	256	383
	TA	2	1,706	120	1,615
	TB	3	163	1,634	160
	TA	8	143	79	35
	TB	9	25	51	3
March 2018	TB	1	13,192	173	489
	TA	2	1,802	19	118
	TB	3	43	31	71
	TA	8	1	8	49
	TB	9	3	21	55

Table 9: Mesozooplankton displacement volumes (DV in mL m^{-3}) and corresponding mesozooplankton biomass in carbon (µg C L^{-1}).

	Transect	Site ID	DV mL m^{-3}	C Biomass µg C L^{-1}
July/August 2017	L	1	0.160	3.36
	L	3	0.281	5.90
	M	1	0.109	2.29
	M	3	0.184	3.86
		Ave	**0.183**	**3.85**
		SD	0.072	1.51
October 2017	TB	1	0.303	6.36
	TA	2	0.363	7.63
	TB	3	0.203	4.27
	TA	8	0.172	3.61
	TB	9	0.133	2.80
		Ave	**0.235**	**4.93**
		SD	0.095	2.00
January 2018	TB	1	0.339	7.12
	TA	2	0.114	2.40
	TB	3	0.165	3.46
	TA	8	0.081	1.69
	TB	9	0.276	5.80
		Ave	**0.195**	**4.09**
		SD	0.109	2.30
March 2018	TB	1	0.259	5.45
	TA	2	0.214	4.49
	TB	3	0.203	4.27
	TA	8	0.156	3.27
	TB	9	0.187	3.92
		Ave	**0.204**	**4.279**
		SD	0.038	0.800

Table 10: Mesozooplankton abundances (ind m^{-3}) showing major taxa and groups present at each experimental site. Also listed are contributions from *Trichodesmium* spp. (counts represent colonies, mostly tufts) and varying sarcodines (mainly acantharia), which occasionally showed up in significant numbers within the tows. Fish eggs were enumerated but not included with the total zooplankton count.

	JULY/AUGUST (ind m^{-3})				**OCTOBER (ind m^{-3})**					**JANUARY (ind m^{-3})**					**MARCH (ind m^{-3})**				
	L1	L3	M1	M3	TB1	TA2	TB3	TA8	TB9	TB1	TA2	TB3	TA8	TB9	TB1	TA2	TB3	TA8	TB9
Copepods	454	11	15	18	36	16	25	55	51	20	6	20	42	72	29	51	7	38	41
Other Crustaceans	0	0	0	0	0	1	0	0	0	3	0	1	1	0	0	0	1	0	0
Cnidarians	0	0	0	1	27	5	8	6	2	4	1	3	6	6	0	3	2	0	2
Chaetognaths	7	3	3	0	14	9	4	6	2	0	2	2	6	6	1	3	9	0	4
Molluscs	2	0	0	0	2	0	1	0	2	1	0	1	0	0	1	0	1	0	1
Tunicates	11	7	3	5	62	33	22	25	9	10	10	6	11	18	7	17	8	3	3
Polychaets	5	0	0	2	2	6	0	0	0	3	1	1	1	2	4	2	0	0	1
Invertebrate Larvae	0	0	0	1	14	1	3	5	8	6	10	17	9	12	5	4	2	1	2
Others	5	3	2	1	7	4	1	1	0	1	1	5	0	0	0	5	5	0	0
Total Zooplankton	485	23	24	29	163	76	63	97	73	47	31	56	76	117	46	85	35	44	55
Fish Eggs	5	1	0	0	38	0	9	0	1	3	1	30	0	6	20	103	2	1	2
Sarcodines	0	58	27	16	122	12	36	25	46	11	7	26	36	94	5	5	7	4	7
Trichodesmium spp.	1	88	2	74	3	0	11	9	8	5	6	3	5	4	0	4	3	0	0

Table 11A: Average ingestion rates (IR) for Chl-*a* (µg chl-*a* cop^{-1} d^{-1}) and cells ingested (cells cop^{-1} d^{-1}). IRs are listed for each of the major taxonomic groups (ciliates, diatoms and dinoflagellates) and for total cells ingested. All values are averages (Ave) from triplicate bottles with their standard deviation (±SD). Note: Negative IRs (no detection of grazing) were excluded and missing SD values indicate less than 3 observations.

	Exp Locations		**Chl *a***		**Ciliates**		**Diatoms**		**Dinoflagellates**		**Total cell abund**	
			µg cop^{-1} d^{-1}		**cells cop^{-1} d^{-1}**		**cells cop^{-1} d^{-1}**		**cells cop^{-1} d^{-1}**		**cells cop^{-1} d^{-1}**	
	Transect	**Site ID**	Ave	± SD	Ave	± SD	Ave	± SD	Ave	± SD	Ave	± SD
July/August 2017	L	1	1.43						78	29	37	14
	L	3			39	25	757	739	204	135	1,001	883
	M	1	0.08	0.04	24	23	150		213	250	467	596
	M	3					3	2	0			
October 2017	TB	1	0.14		457	199			671	163	681	172
	TA	2	0.66		244	40	3,515	616			3,909	602
	TB	3	0.59	0.32	322	248	2,499	223	192	61	3,034	259
	TA	8	0.23		309		61		100	7	270	
	TB	9	0.35		41	59	28	5	78	65	120	
January 2018	TB	1	0.26		781		3,624	1,529	2,220	946	6,112	2,540
	TA	2	10.55	6.26	252		5,356		11,619		15,922	
	TB	3	1.06	0.20	1,237	895	154		165	113	930	364
	TA	8	0.12		292	103	525	239	98		801	363
	TB	9	0.40	0.21	438	569	105	87	53	15	130	66
March 2018	TB	1	3.53		1,932	2,323	3,783		2,202		4,370	
	TA	2	3.20	1.84	289	339			347	126		
	TB	3	0.02		121		404		175	150	987	
	TA	8	0.46		202	122	44		411	461	218	164
	TB	9	0.01		77	50	42	7	51	5	142	15

Table 11B: Carbon IR (µg C cop^{-1} d^{-1}) for each of the major taxonomic groups and total C combining all prey categories. Values are averages (Ave) from triplicate bottles with their standard deviation (±SD). Note: Negative IRs were excluded and missing SD values indicate less than 3 observations.

	Locations		**Ciliates** µg C cop^{-1} d^{-1}		**Diatoms** µg C cop^{-1} d^{-1}		**Dinoflagellates** µg C cop^{-1} d^{-1}		**Total C** µg C cop^{-1} d^{-1}	
	Transect	**Site ID**	Ave	± SD	Ave	± SD	Ave	± SD	Ave	± SD
	L	1					3.23	1.2	2.66	0.9
July/August 2017	L	3	0.19	0.1	22.14	21.4	2.62	1.7	24.95	23.1
	M	1	0.12	0.1	3.51		5.68	6.7	8.12	9.9
	M	3			0.03	0.0	0.01		0.01	
	TB	1	41.87	16.7			21.20	5.2	52.04	9.6
	TA	2	4.81	0.8	128.29	34.0			84.63	17.1
October 2017	TB	3	9.67	2.6	48.30	11.6	13.73	2.7	71.70	15.4
	TA	8	9.84		2.34		3.09	0.2	10.92	14.9
	TB	9	0.85	1.1	0.92	0.2	1.07	1.0	2.35	2.4
	TB	1	19.25		151.24	59.0	31.31	13.3	194.29	87.5
	TA	2	13.13		187.41		122.67		168.16	
January 2018	TB	3	84.58	25.4	4.47		2.92	2.0	90.19	27.7
	TA	8	7.13	0.9	14.00	7.0	2.46		22.75	6.6
	TB	9	9.77	11.9	1.08	1.6	0.63	0.1	11.49	13.7
	TB	1	17.54	17.3	207.40		28.50		101.79	115.3
	TA	2	3.56	2.2			18.65	6.8	31.18	
March 2018	TB	3	3.81		14.90		3.97	3.4	10.76	14.9
	TA	8	3.79	2.4	0.37		8.39	9.4	11.13	9.7
	TB	9	1.25	0.5	0.12	0.0	0.77	0.1	2.14	0.5
Ave			13.60		49.16		15		47.43	
SD			20.94		73.97		29		57.48	

Table 12: Average values (Ave) with their standard deviation (SD) for IR for chl-*a* (µg chl-*a* cop^{-1} d^{-1}) , cells ingested (cells cop^{-1} d^{-1}), and carbon (µg C cop^{-1} d^{-1}) listed for major groups (ciliates, diatoms and dinoflagellates) and for total IR grouped by season and by location (distance to shore). N = total number of observations for average calculations

Season	n	Chl *a* µg cop^{-1} d^{-1}		Ciliates cells cop^{-1} d^{-1}		Diatoms cells cop^{-1} d^{-1}		Dinoflagellates cells cop^{-1} d^{-1}		Total cell abund cells cop^{-1} d^{-1}		Ciliates µg C cop^{-1} d^{-1}		Diatoms µg C cop^{-1} d^{-1}		Dinoflagellates µg C cop^{-1} d^{-1}		Total C µg C cop^{-1} d^{-1}	
		Ave	SD	Ave	SD	Ave	SD	Ave	SD	Ave	SD	Ave	± SD	Ave	± SD	Ave	± SD	Ave	± SD
July/August 2017	12	0.4	0.7	32	23	323	541	149	157	502	677	0.1	0.1	9.2	15.8	3.1	3.7	9.7	15.2
October 2017	15	0.5	0.3	272	214	2,018	1,582	260	264	1,948	1,660	13.7	17.2	59.3	58.4	9.8	8.9	46.7	35.3
January 2018	15	3.1	5.2	613	644	1,536	2,034	1,594	3,320	3,065	4,668	28.4	34.7	57.9	80.4	19.3	35.5	92.3	104.5
March 2018	15	0.2	0.3	553	1,190	726	1,504	525	763	1,201	1,975	6.1	9.3	37.2	83.6	10.9	11.1	31.4	62.7
Distance to Shore (km)																			
0 - 50	33	2.1	3.5	586	939	2,442	1,801	1,045	2,275	2,846	3,535	20.7	28.0	88.1	77.0	17.8	23.9	73.9	83.3
100+	24	0.3	0.2	194	255	235	392	137	199	410	494	4.0	5.8	6.1	11.5	2.5	4.0	11.2	13.2

Table 13: Results of one-way ANOSIM comparing C-based IRs for ciliates, diatoms, dinoflagellates and total cell IRs across season and distance to shore a. All global tests were run at 9999 permutations. *R* = sample statistic. P = significance level

Prey	Season		Distance from Shore	
	R	P	*R*	P
Ciliates	0.192	0.0001		NS
Diatoms	0.047	0.038		NS
Dinoflagellates		NS	0.091	0.016
Total	0.116	0.0001	0.067	0.042

Table 14: Results of two-way ANOSIM examining the effect of distance to shore and presence/absence of copepods (Cop Pres/Abs) on prey community structure at the end of each experiment. All global tests were run at 9999 permutations. *R* = sample statistic. P = significance level.

Season	Distance		Cop Pres/Abs	
	R	P	*R*	P
July/August 2017	0.407	0.0004		NS
October 2017	0.852	0.0001	0.211	0.006
January 2018	0.636	0.0001		NS
March 2018	0.714	0.0001		NS

Table 15A: Average values (Ave) with their standard deviation (SD) for % biomass removed for carbon listed for major groups (ciliates, diatoms and dinoflagellates) and for total C grouped by season and by location (distance to shore). N = total number of observations for average calculations.

		Ciliate C	**Diatom C**	**Dino C**	**Total C**
			%		
JULY/AUGUST	L1	0.00	0.00	502.87	502.9
	L3	0.52	71.39	1.24	73.2
	M1	0.00	29.29	31.01	60.3
	M3	0.00	0.00	0.86	0.9
Ave		0.1	25.2	134.0	159.3
Min		0.0	0.0	0.9	0.0
Max		0.52	71.4	502.9	502.9
OCTOBER	TB1	18.69	0.00	19.43	38.1
	TA2	14.42	7.45	0.00	21.9
	TB3	4.01	8.92	5.43	18.4
	TA8	203.80	100.84	29.18	333.8
	TB9	8.76	17.40	24.41	16.9
Ave		49.94	26.92	15.69	85.81
Min		4.01	0.00	0.00	0.00
Max		203.80	100.84	29.18	203.80
JANUARY	TB1	13.25	16.89	14.41	44.5
	TA2	6.97	6.99	4.83	18.8
	TB3	5.95	3.15	2.09	11.2
	TA8	44.02	47.47	34.01	125.5
	TB9	166.01	37.17	158.52	120.6
Ave		47.24	22.33	42.77	64.12
Min		5.95	3.15	2.09	2.09
Max		166.01	47.47	158.52	166.01
MARCH	TB1	14.94	2.31	8.57	25.8
	TA2	46.91	0.00	40.31	87.2
	TB3	4.53	12.70	2.06	19.3
	TA8	116.60	128.28	44.10	289.0
	TB9	16.59	9.84	3.84	10.1
Ave		39.92	30.63	19.78	86.28
Min		4.53	0.00	2.06	0.00
Max		116.60	128.28	44.10	128.28

Table 15B: Average values (Ave) and ranges for listed percentage of prey standing stocks (C) removed by natural abundances of copepods for major groups (ciliates, diatoms and dinoflagellates) and for total percent removed grouped by season and by location (distance to shore). N = total number of observations for average calculations

Season	**n**	**Ciliate C**		**Diatom C**		**Dino C**		**Total C**	
		Ave	Range	Ave	Range	Ave	Range	Ave	Range
July/August 2017	4	0.13	0 - 0.52	25.2	0 - 71	134.0	0.86 - 503	159.3	0-503
October 2017	5	49.9	4.01 - 204	26.9	0 - 101	15.7	0 - 29	92.6	0-204
January 2018	5	47.2	5.95 - 166	22.3	3.15 - 48	42.8	2.09 - 159	112.3	2.09-166
March 2018	5	39.9	4.53 -117	30.6	0 - 128	19.8	2.06 - 44	90.3	0-128
Distance to Shore (km)									
0 - 50	11	11.8	0 - 47	8.0	0 - 29	57.37	0 - 503	77.13	0-503
100 +	8	69.5	0 - 204	51.6	0 - 128	37.02	0.86 - 159	158.11	0-159

Table 16: Average relative contributions (% C) from ciliates, diatoms and dinoflagellates to copepod diet grouped by season and location. Averages were only calculated when grazing could be detected (exclusion of negative IRs).

Season	**Ciliates** % Ave	**Diatoms** % Ave	**Dinoflagellates** % Ave
July/August 2017	0.5	51.8	47.7
October 2017	35.6	42.3	22.1
January 2018	44.2	41.3	14.5
March 2018	25.7	31.2	43.1
Distance to Shore (km)			
0 - 50	20.9	44.3	34.8
100+	37.4	20.3	25.8

Figures

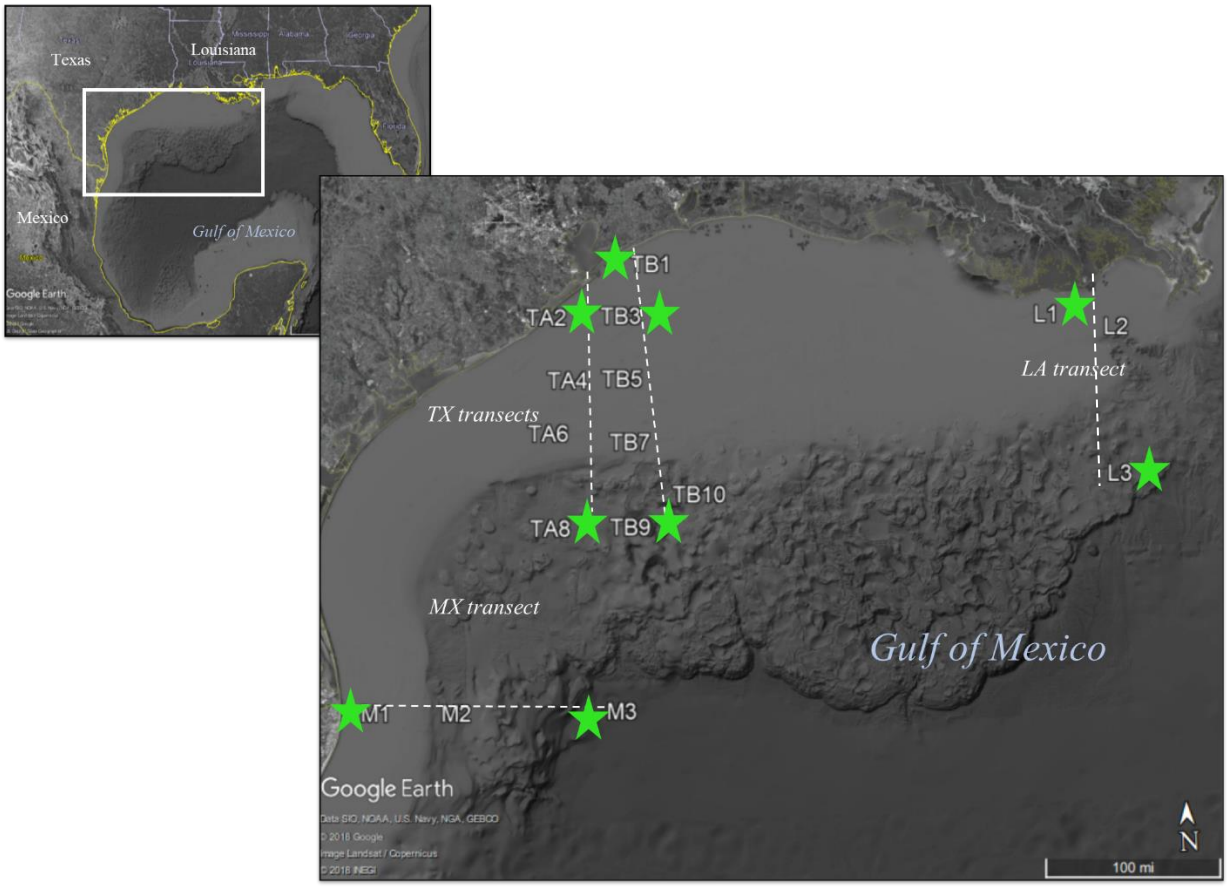

Figure 1: Map of the study region within the northern Gulf of Mexico. Sampling occurred along varying transects (dashed lines) off the Louisiana (L), Texas (TA and TB) and Mexico coasts (M). Water samples were collected for biological, physical and chemical measurements (all stations) and feeding experiments conducted at a subset of the sites (star symbols).

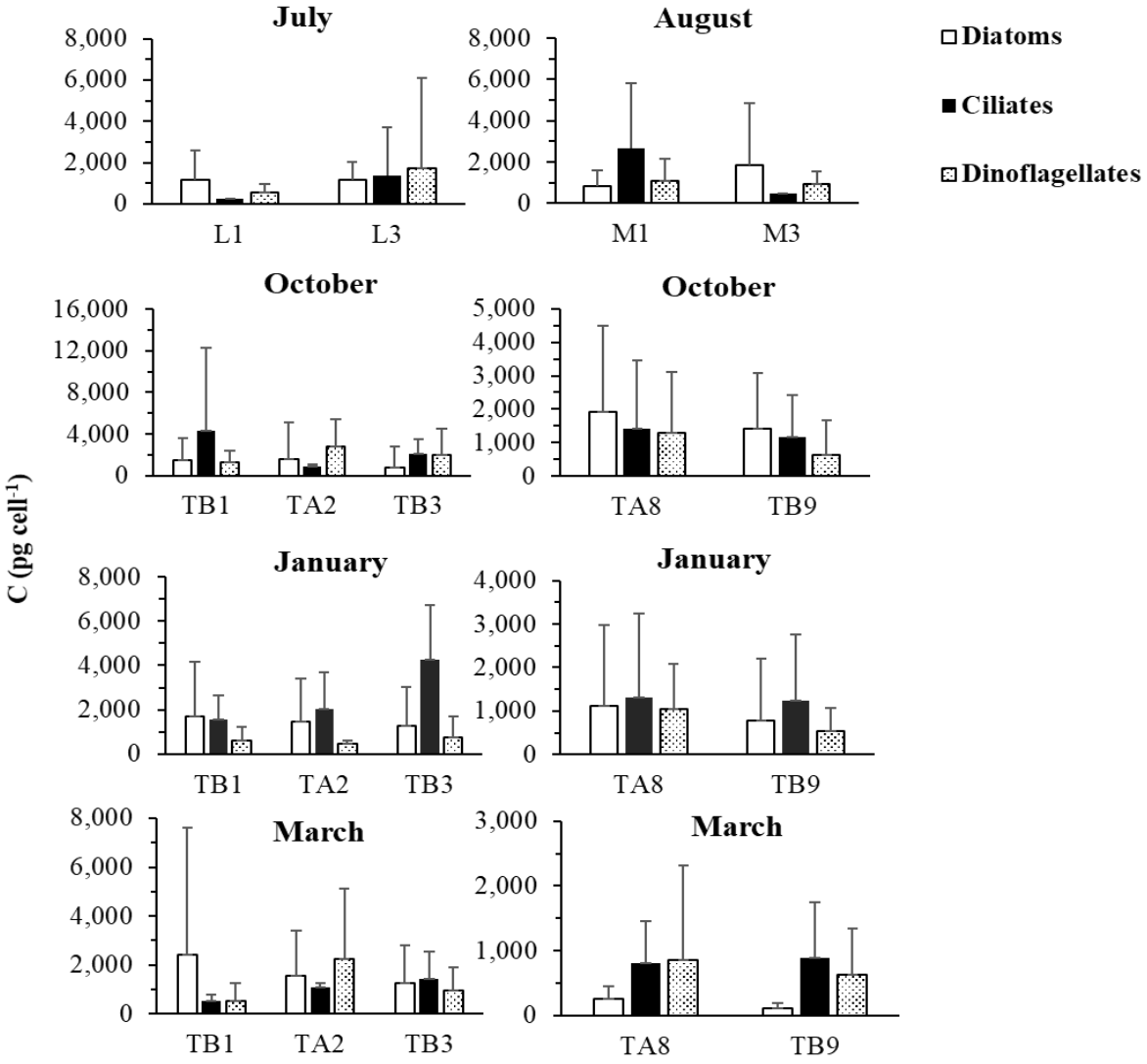

Figure 2: Average cell carbon content for diatoms, ciliates and dinoflagellates in initial seawater samples (pg C $cell^{-1}$) for each cruise period and station shown with their standard deviation (±SD). Details on station information see Table 1 and Fig. 1.

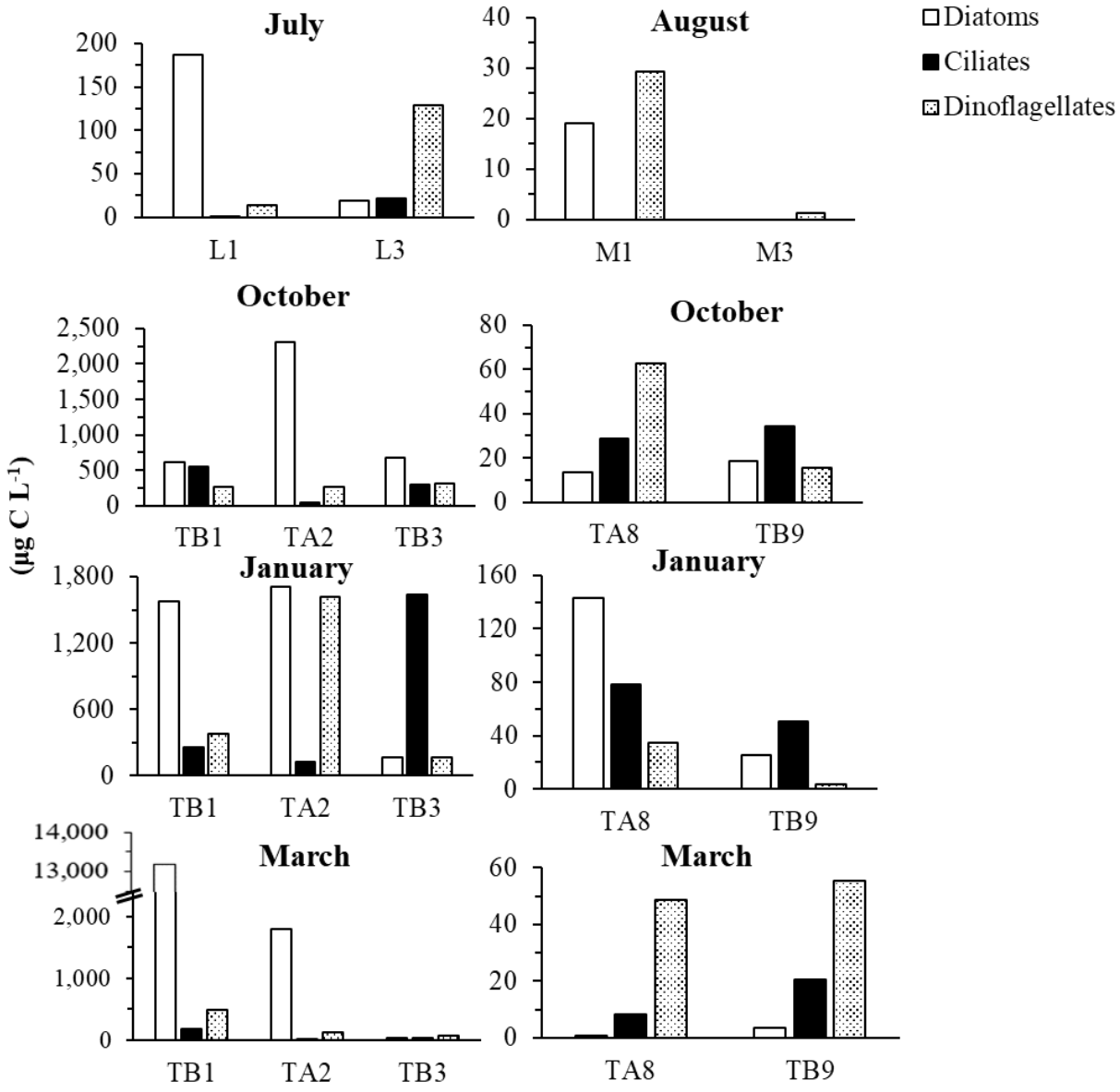

Figure 3: Carbon biomass (µg C L^{-1}) in initial seawater samples for all feeding experiments.

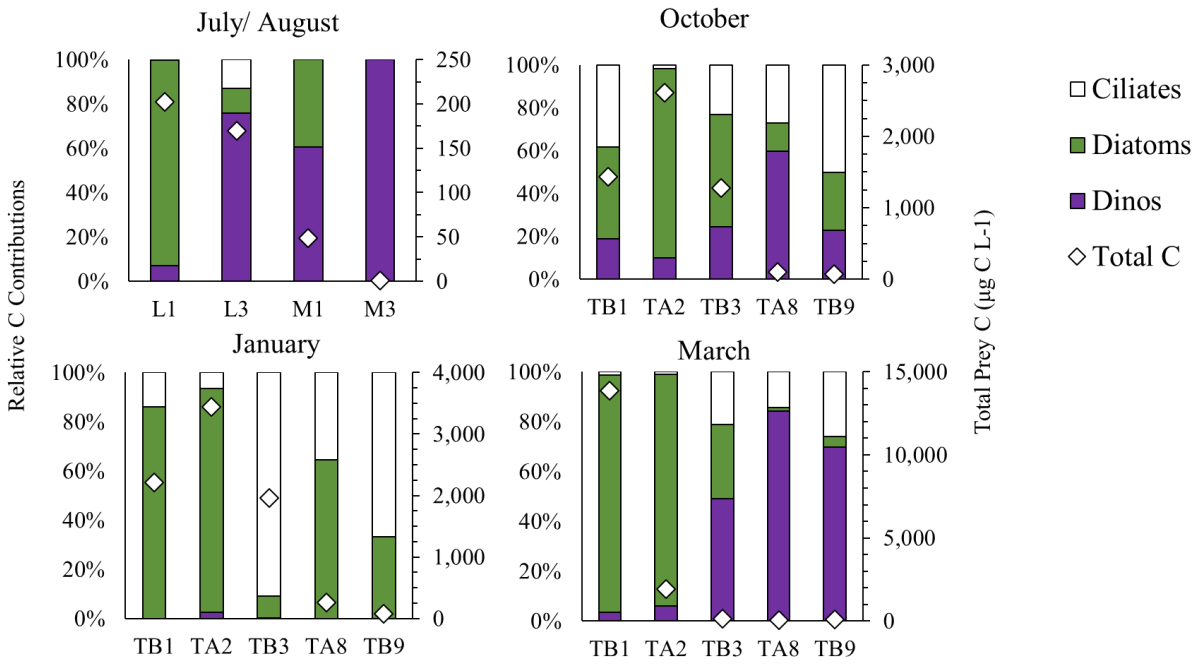

Figure 4: Relative contributions of the differing microeukaryote groups to the total assemblage (% C) during each of the seasons and at each station (primary y-axes). Also depicted is total C biomass (µg L^{-1}, secondary y-axes). Note varying scales on secondary y-axes.

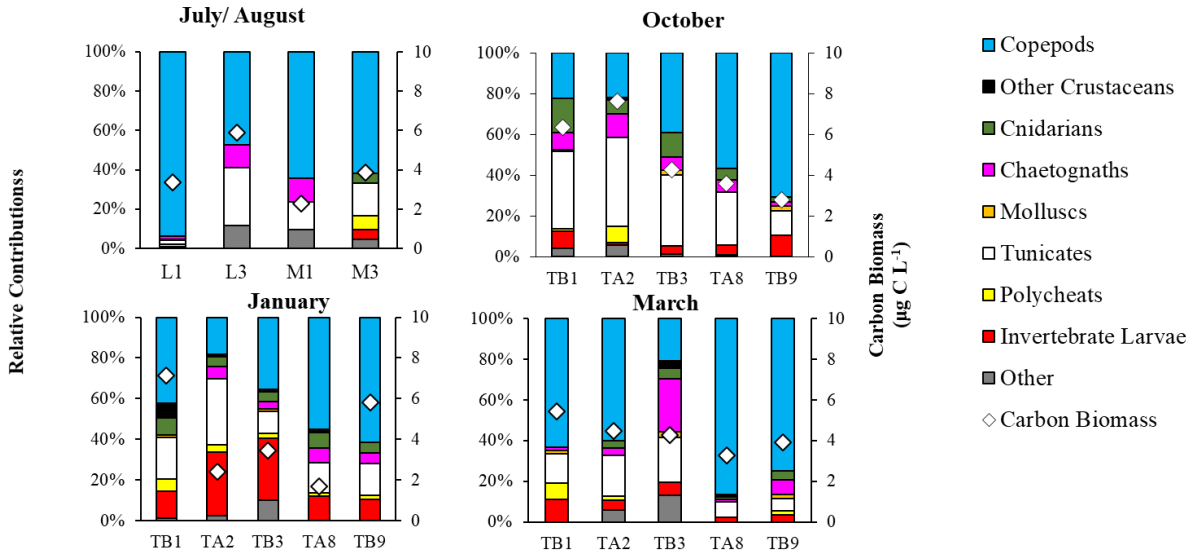

Figure 5: Relative contributions of differing zooplankton taxa to the overall assemblage for each season and at each station (primary y-axes). The total C biomass of the zooplankton assemblage is also shown (secondary y-axes).

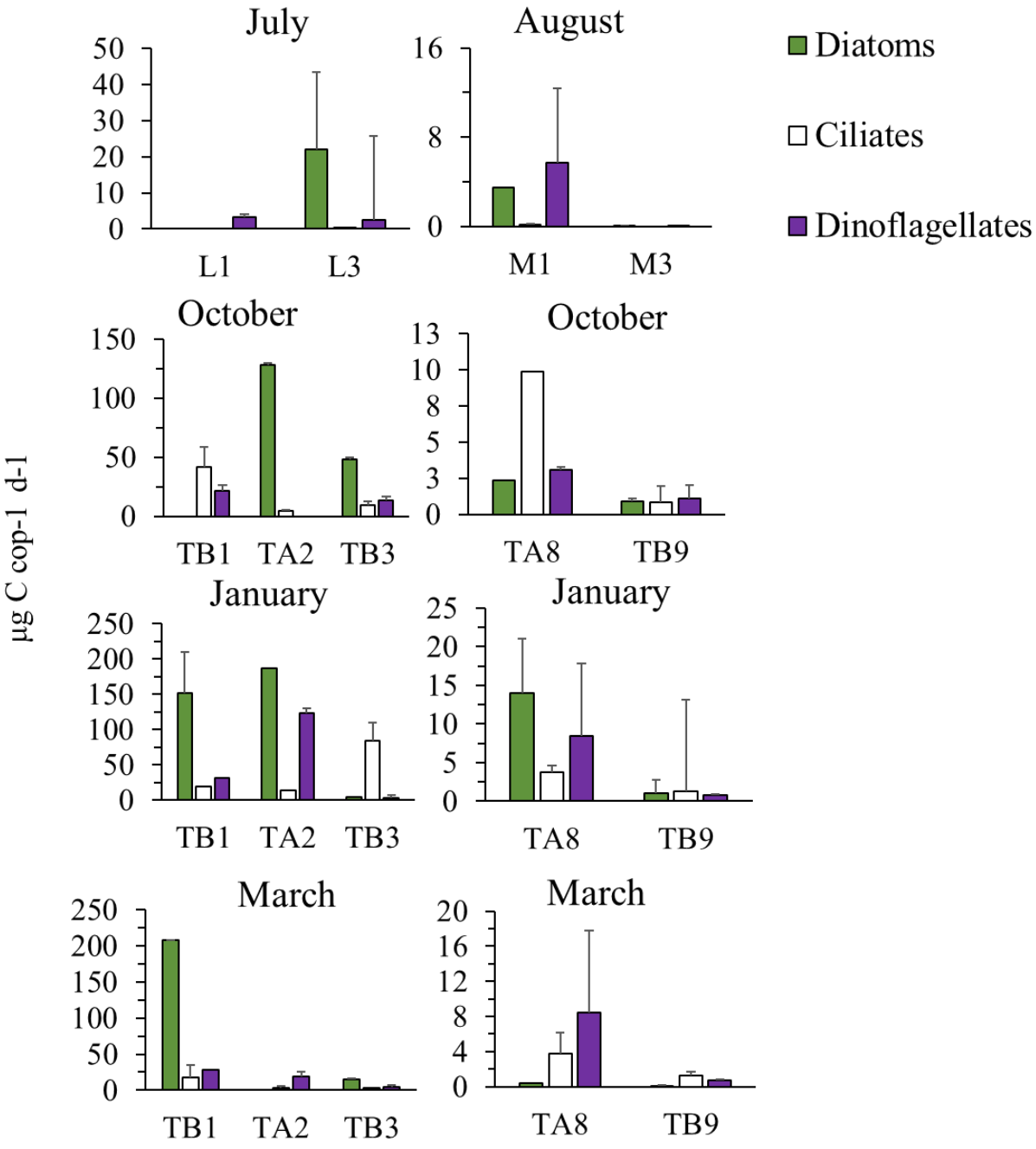

Figure 6: Carbon IR (µg C cop^{-1} d^{-1}) for each of the major taxonomic groups. Values are averages (Ave) from triplicate bottles with their standard deviation (±SD). Note: Negative IRs excluded.

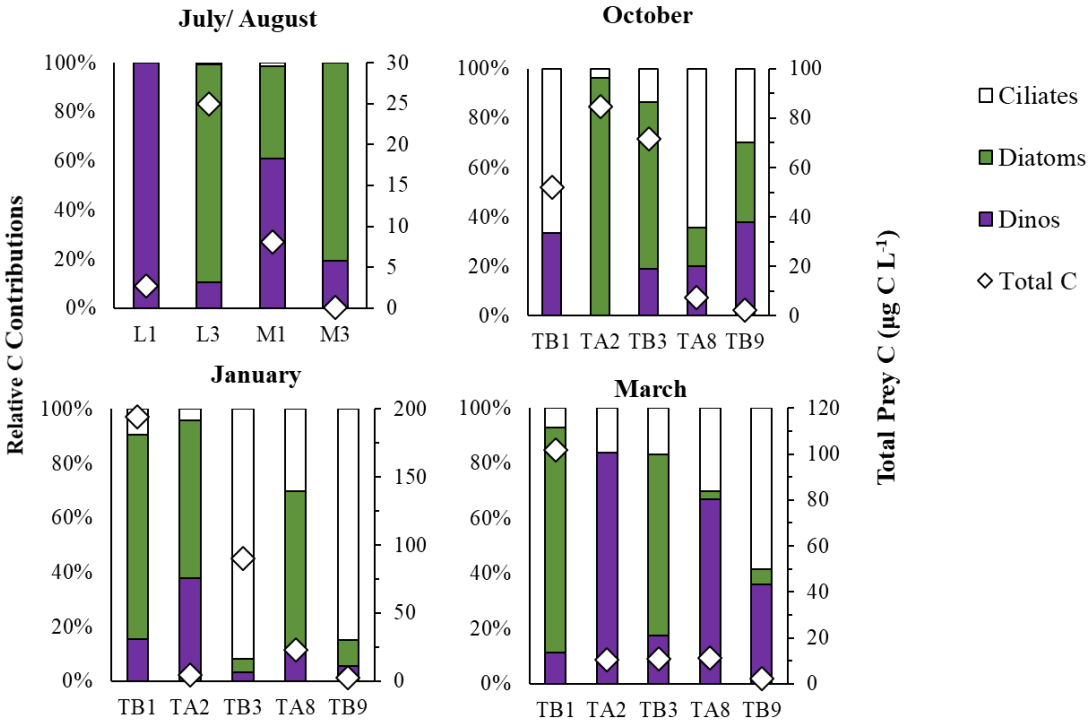

Figure 7: Relative contributions from prey biomass groups to copepod diet during each of the seasons and at onshore (L1, M1, TB1, TA2 and TB3) and offshore stations (L3, M3, TA8 and TB9).

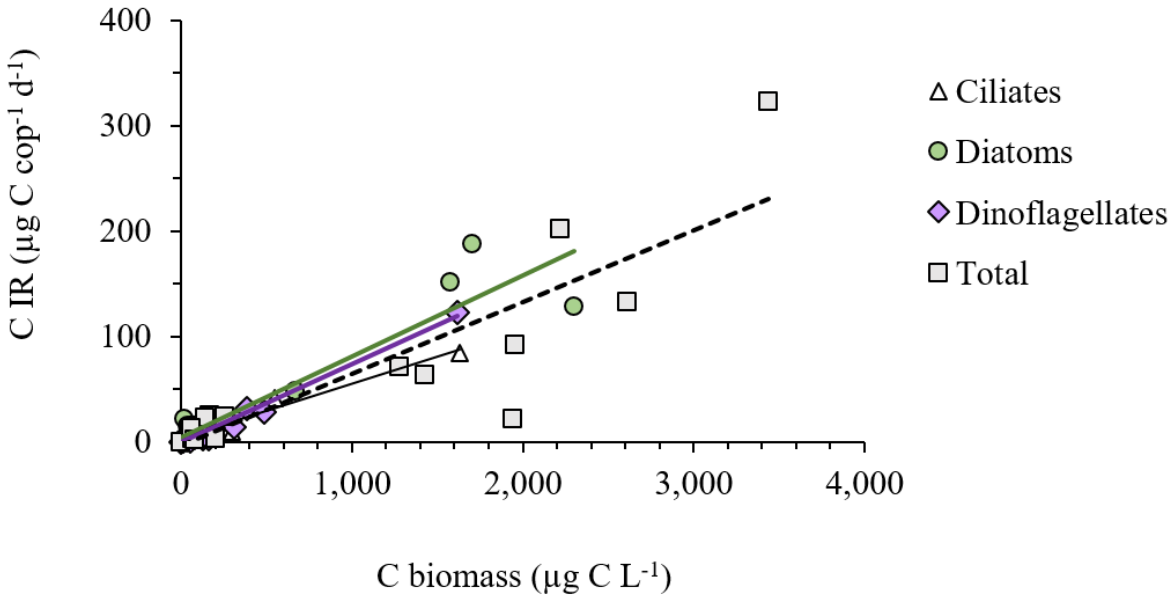

Figure 8: Relationship between IRs (µg C cop^{-1} d^{-1}) and prey abundance for each prey type and total carbon (µg C L^{-1}). Averages were only used when grazing could be detected (exclusion of negative IRs).

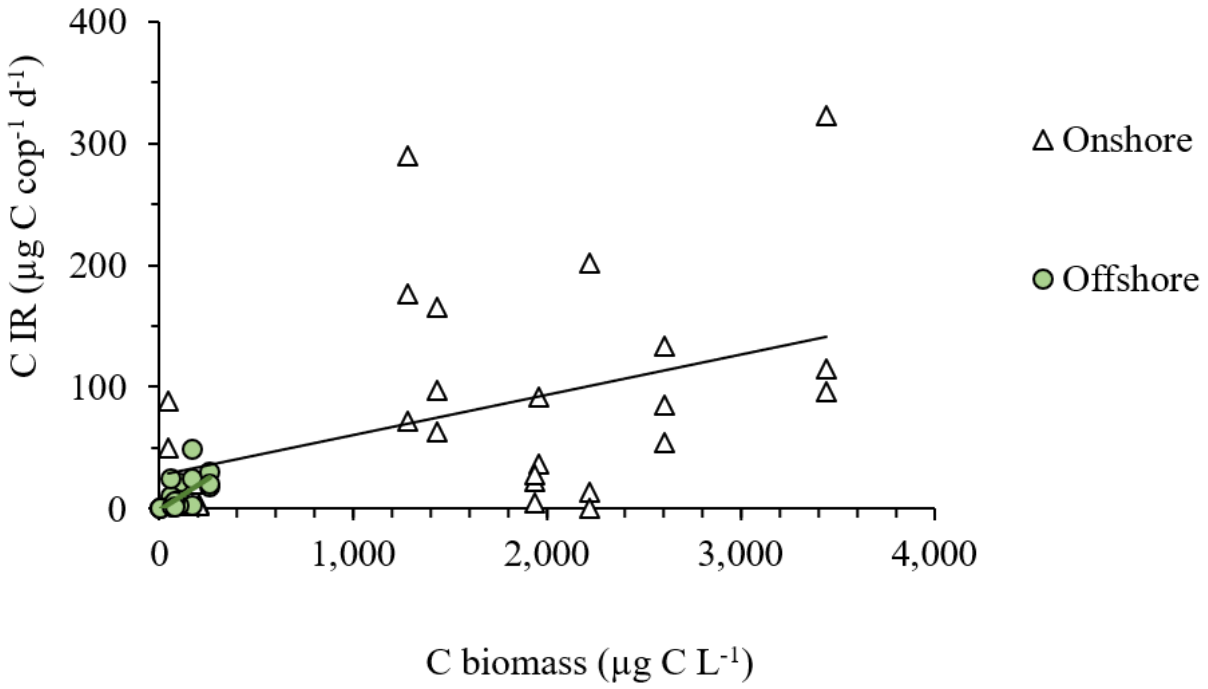

Figure 9: Relationship between IRs (µg C cop-1 d-1) and total prey C (µg C L^{-1}) depicting onshore and offshore sites. Note: negative IRs were not included